

## **Supporting Information for**

# **Dynamic Fluidic Manipulation in Microfluidic Chips with Dead-End Channels Through Spinning: The Spinochip Technology for Hematocrit Measurement, White Blood Cell Counting and Plasma Separation**

Cemre Oksuz<sup>1</sup>, Can Bicmen<sup>2</sup>, H. Cumhuri Tekin<sup>1,3,4\*</sup>

<sup>1</sup>Department of Biotechnology and Bioengineering, Izmir Institute of Technology, Izmir 35430, Turkiye

<sup>2</sup>Department of Medical Microbiology, Dr. Suat Seren Training and Research Hospital for Chest Diseases and Chest Surgery, Izmir 35430, Turkiye

<sup>3</sup>Department of Bioengineering, Izmir Institute of Technology, Izmir 35430, Turkiye

<sup>4</sup>METU MEMS Center, Ankara 06520, Turkiye

\*Corresponding author E-mail: cumhurtekin@iyte.edu.tr

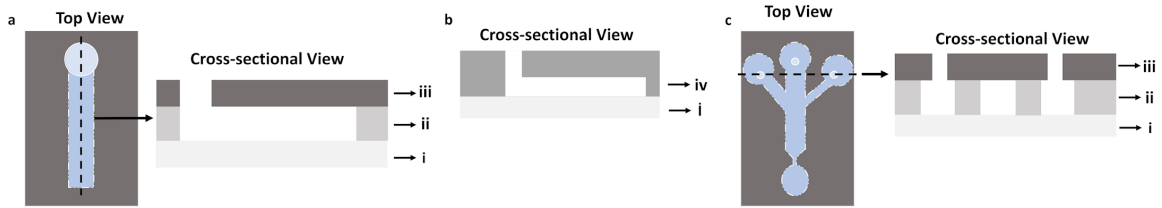


**Fig. S1.** Top and cross-sectional views of Spinochip devices. Dead-end straight channels fabricated using a) PMMA and b) PDMS. c) A dead-end channel with three reservoirs for programmable filling experiments. Spinochip devices can contain different layers: i) a glass slide, ii) DSA layer, iii) PMMA layer or iv) PDMS layer containing reservoir(s).

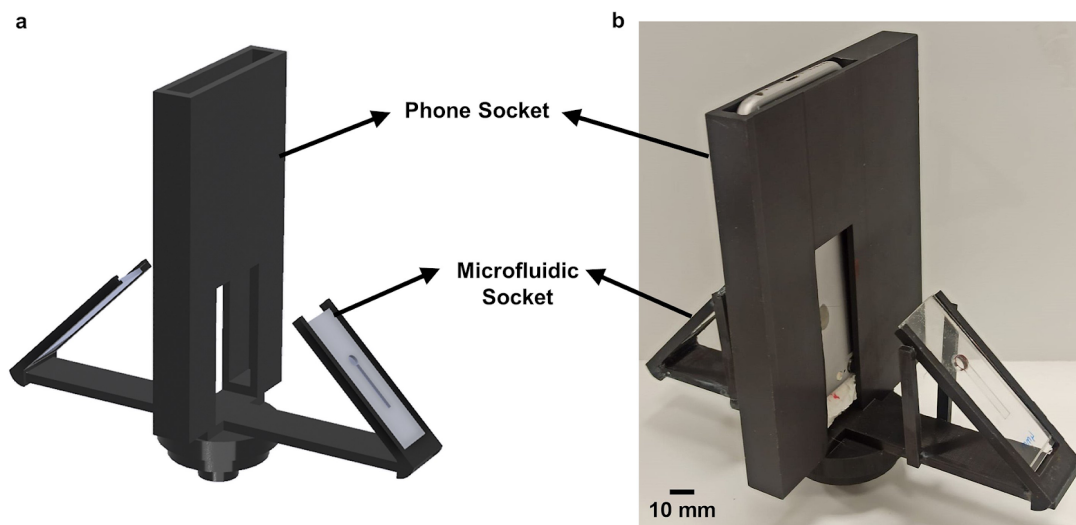


**Fig. S2.** Rotating platform with phone socket. a) The illustration of rotating platform contains two microfluidic sockets and one phone socket. b) Photograph of the rotating platform. The platform was mounted on a spin coater (Midas, Spin Process Controller) for experiments conducting at different spinning speeds. A smart phone was used for monitoring the channel during spinning.

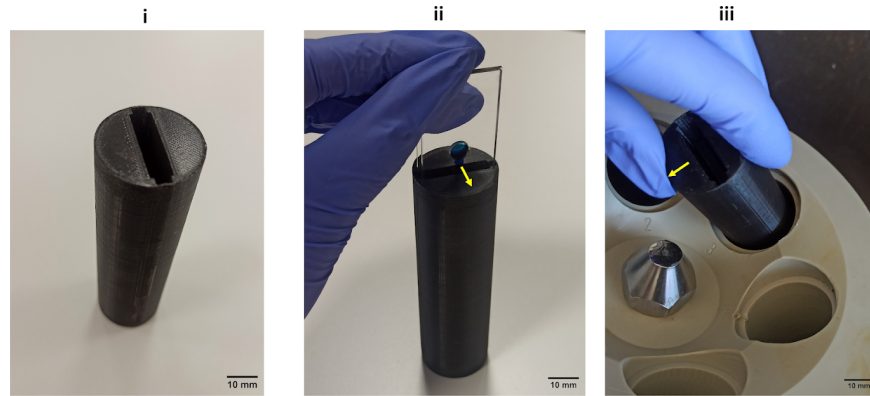


**Fig. S3.** Apparatus for using Spinochip devices in a centrifuge device, which can process 50 mL centrifuge tubes. The apparatus has an opening (i) to place a Spinochip device tightly (ii). For centrifugation, the apparatus is placed into rotor of the centrifuge (iii) with the reservoir of the Spinochip device facing the center of the rotor.

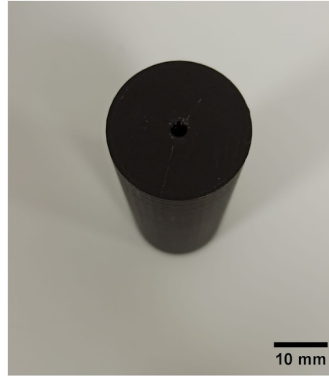


**Fig. S4.** Microhematocrit apparatus for hematocrit measurement using a microhematocrit tube inside a centrifuge device.

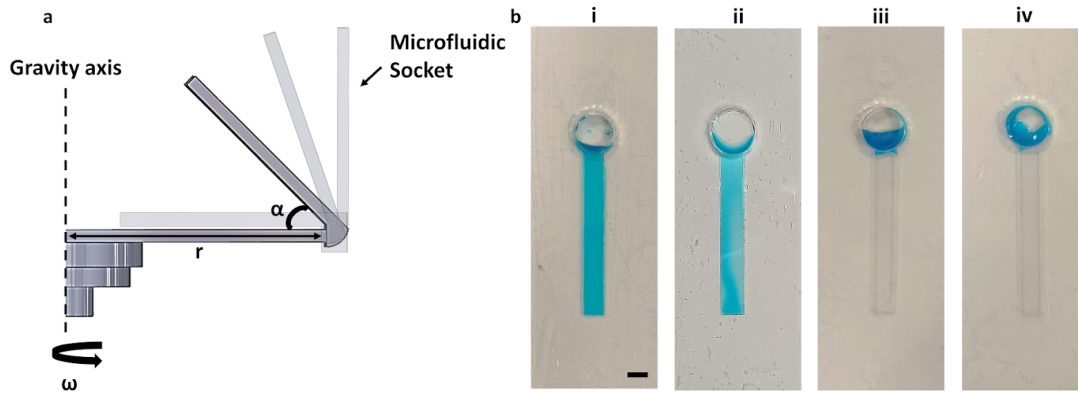


**Fig. S5.** Testing of sockets with different angles ( $\alpha$ ). a) The illustration of rotating platform with different angles. b) Filling of channels ( $3 \text{ mm} \times 25 \text{ mm} \times 0.15 \text{ mm}$  ( $w \times L \times h$ )) using different socket angles: i)  $0^\circ$ , ii)  $45^\circ$ , ii)  $60^\circ$  and iii)  $90^\circ$  at a rotation speed of 400 rpm for 2 min. Scale bar is 3 mm.

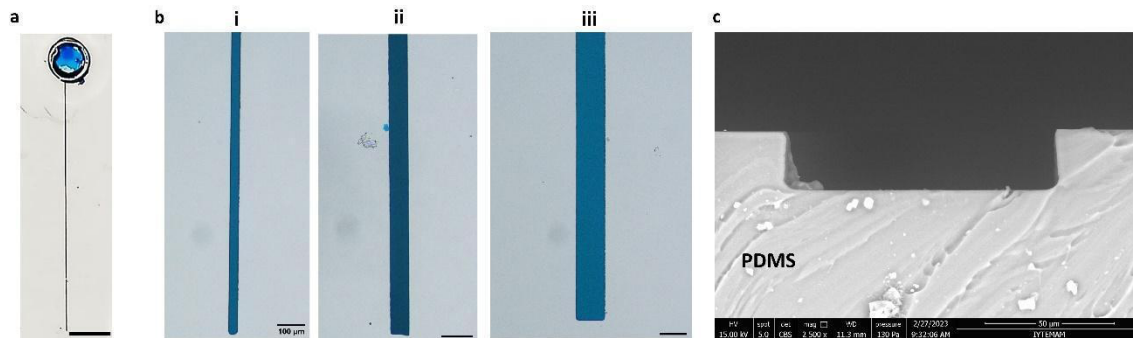


**Fig. S6.** The filling tests of PDMS microfluidic chips. a) A PDMS microfluidic chip containing a dead-end channel and a reservoir. Scale bar is 2 mm. b) Microscope images of filled PDMS chips with same height (30 μm) and length (1.8 mm), but different widths: i) 30μm, ii) 50μm and iii) 100 μm. Channels were filled at a rotation speed of 3000 rpm for 10 min. Scale bars are 100 μm. c) SEM image of a PDMS chip with 100 μm channel width.

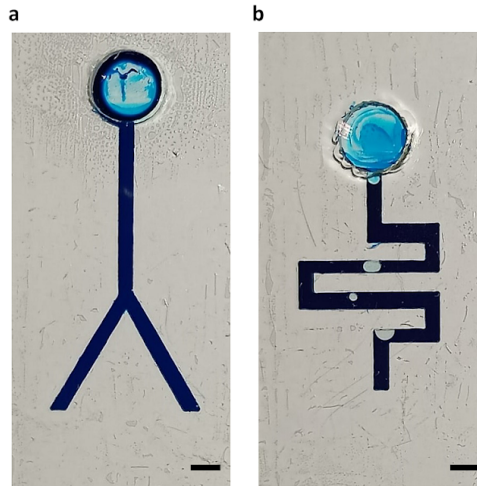


**Fig. S7.** Filling of different channel geometries. a) Y-shaped and b) serpentine channels with a single reservoir. Filling of channels at a rotation speed of 1000 rpm for 5 min. Scale bar is 2 mm.

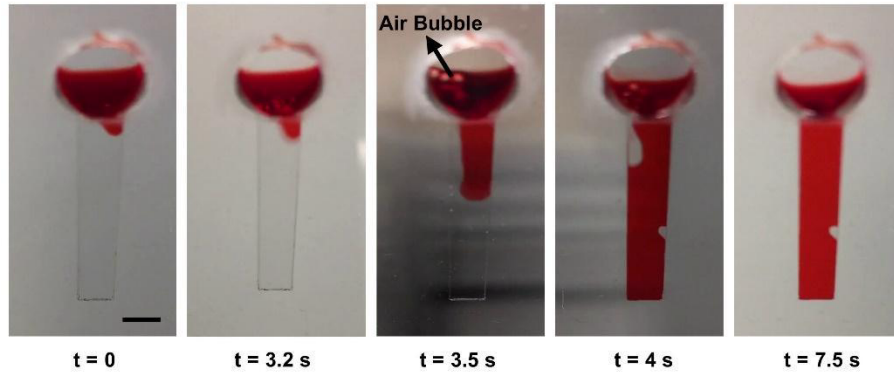


**Fig. S8.** The rapid filling of a channel having 3 mm width, 0.15 mm height, and 25 mm length. At  $t=3.2$  s, the air burst occurs, releasing the trapped air into the reservoir and leading to a rapid filling of the channel. Before this moment, according to Boyle's Law, the internal air pressure inside the channel rises to  $1.037 \pm 0.014$  atm. Following the burst, by  $t=3.2$  s, a rapid filling profile is observed, and by  $t=7.5$  s, the channel is completely filled. Scale bar is 3 mm.

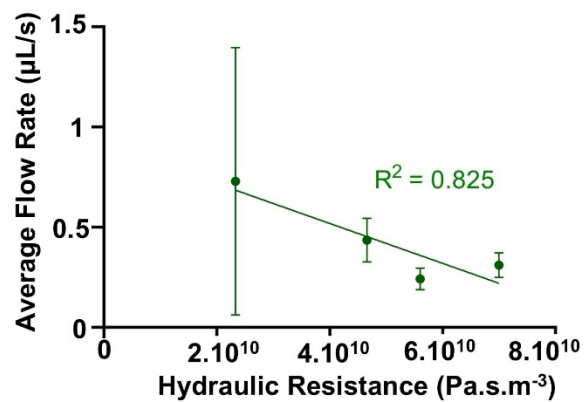


**Fig. S9.** Flow rate for channels of varying lengths (12, 25, 30, and 37.5 mm), each with a width of 2 mm and a height of 150 µm. 500 rpm was used to fill the channels.

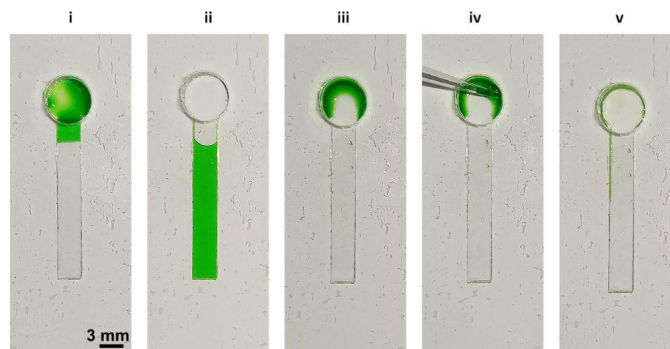


**Fig. S10.** Fluid manipulation in Spinochip. Sequential fluidic manipulation: (i) The solution was introduced in the reservoir and then (ii) it was filled into channel at 400 rpm for 2 min. Afterwards, Spinochip was turned upside down and (iii) centrifuged 500 rpm for 2 min to collect solution to the reservoir. Lastly, (iv-v) the solution was pipetted out from the reservoir. Scale bar is 3 mm.

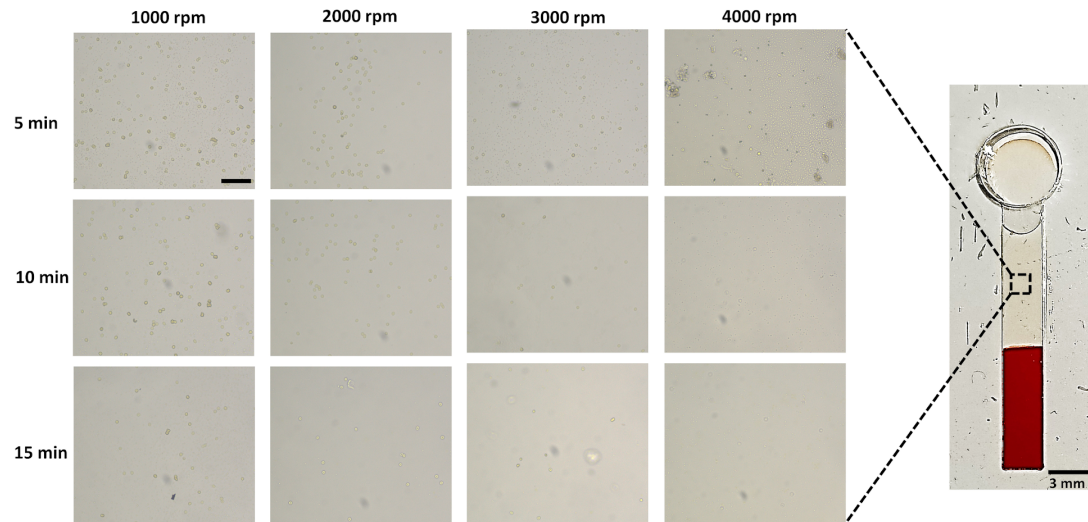


**Fig. S11.** Micrographs of cells remained in the plasma after centrifugation of a Spinochip device at different rotation speeds and durations. Scale bar is 100  $\mu\text{m}$ .

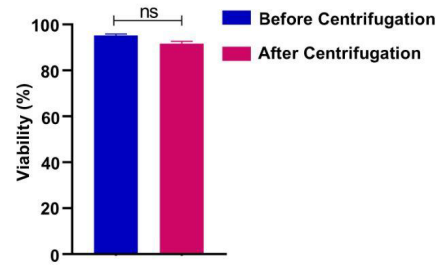


**Fig. S12.** The effect of on-chip centrifugation on cell viability. U-251 human glioblastoma multiforme cell line with a concentration of  $10^4$  cells/mL was used in the experiments. The cells were centrifuged at 4000 rpm for 10 min in the microfluidic chip used for blood analysis. The cells were collected from the reservoir with back-centrifugation presented in Figure S10iii. Cell viabilities were analyzed using a hemacytometer with trypan blue staining. ns represents non-significant,  $p>0.05$ .

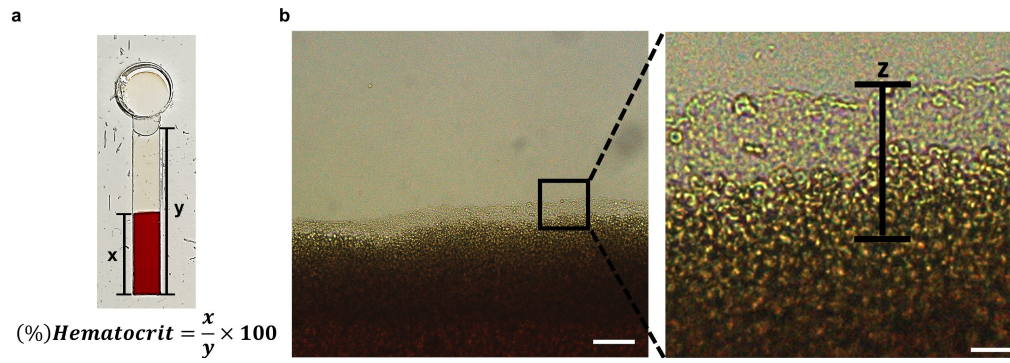


**Fig. S13.** Hematocrit and white blood cell measurement in Spinoclip. a) Hematocrit value measured by dividing the thickness of RBC ( $x$ ) by the thickness of blood ( $y$ ) in a channel. b) White blood cell concentration measured by measuring the thickness of buffy coat ( $z$ ). Scale bar is 100  $\mu\text{m}$ .

**Video S1 (separate file).** Filling of a dead-end channel with spinning with 20  $\mu\text{L}$  of food dye at 500 rpm spinning. During spinning, the air entrapped within the channel, leading to pressurization. As air pressure steadily increases, air escapes towards the reservoir as bubbles due to the pressure difference between the channel and the reservoir. This fundamental process iterates until the channel is completely filled.

**Video S2 (separate file).** Sequential filling of a microfluidic chip from different reservoirs. 4  $\mu\text{L}$  of food dyes with distinct colors were given into the reservoirs and the chip was exposed to 350 rpm, 500 rpm and 700 rpm spinning, respectively, for 30 s each. As a result, different food dyes from reservoirs connected to channels with widths of 4 mm, 2 mm, and 1 mm were successively introduced into the main channel.

**Table S1.** Comparison of centrifugal microfluidic devices for blood separation

Valve	Number of Chip Layers	Vent Port	Special Instrument for Operation <sup>†</sup>	Minimum Sample Volume (μL)	Sample Treatment	Staining for Analysis	Additional Reagents/ Methods Used for Analysis <sup>†</sup>	Analysis Time (min)	Plasma Collection	HCT	WBC	FM <sup>‡</sup>	Ref.
+ (Siphon Valve)	5	+	+ (Servo Motor)	2000	-	-	-	2.5	+	-	-	5×10 <sup>1</sup>	(1)
-	3	+	+ (Spin Processor)	1	+ (Dilution)	-	+ (Zweifach-Fung effect)	~0.1	+/- (Remained on chip)	-	-	8×10 <sup>5</sup>	(2)
-	3	+	-	90	-	-	+ (Cross-flow filtration)	3	+	-	-	1.5×10 <sup>3</sup>	(3)
+ (Centrifugo-Pneumatic Siphon)	6	+	+ (Spindle motor)	18	+ (Dilution)	-	+ (Density-gradient medium)	NR	+	-	- (only separation)	-	(4)
-	2	-	+ (Rotational Platform)	100	-	-	+ (Density-gradient medium, spiral microfluidic channel)	3	-	-	- (only separation)	1×10 <sup>3</sup>	(5)
+ (Capillary and Siphon Valves)	6	+	+ (Commercial centrifugal platform)	10	+ (On-chip Dilution)	+	-	15	+/- (Remained on chip)	+	+	1×10 <sup>3</sup>	(6)
+ (Ferrowax Valves)	3	+	+ (Rotational Platform)	4000	+ On-chip dilution	+	+ (Cell enrichment Cocktail)	10	+/- (Remained on chip)	-	- (only separation)	1	(7)
+ (Capillary Valves)	3	-	+ (DC motor)	10	+ (Dilution)	+	+ (Density-gradient medium)	10	-	-	+	2.1×10 <sup>3</sup>	(8)
-	3	+	+ (Rotational Platform)	10	-	-	+ (Density-gradient medium)	10	+/- (Remained on chip)	+	+	6.4×10 <sup>3</sup>	(9)
-	≥2	-	-	0.1	-	-	-	10	+	+	+	1×10 <sup>7</sup>	This study

<sup>†</sup>: other than a standard bench top centrifuge device

<sup>‡</sup>: other than centrifugation

+/-: Yes/No

NR: not reported

HCT: Hematocrit measurement

WBC: white blood cell concentration measurement

FM: Figure of Merit;  $FM = \frac{(Plasma\ Collection)(HCT)(WBC)}{(Sample\ Volume)(Analysis\ Time)(Vent\ Port)(Layers)(Special\ Instrument)(Sample\ Treatment)(Staining)(Additional\ Reagents/Methods)}$

In FM calculations, qualitative indicators were quantified by assigning numerical values: a positive sign ('+') was assigned a value of 2, a negative sign ('-') was assigned a value of 1, and a mixed sign ('+/-') was assigned a value of 1.5. All figure of merit (FM) values were then normalized relative to the lowest FM value.

**Table S2.** Comparison of microfluidic devices for blood separation

Method for Flow Generation	Number of Chip Layers	Minimum Sample Volume ( $\mu$ L)	Sample Pretreatment	Staining for Analysis	Additional Reagents/ Methods Used for Analysis	Analysis Time (min)	Plasma/ Serum Separation	HCT	WBC	Ref.
Capillary-driven (Paper-based)	2	NR	-	-	On-chip surface treatment/ Naked-eye inspection	30	-	+	-	(10)
Capillary-driven (Paper-based)	3	4	+ (Dilution)	+	Acridine Orange Staining/ Size-based filtration & Smartphone-based inspection	5	-	-	+	(11)
Capillary-driven (Paper-based)	2	15	+ (Lysis and antibody-conjugated gold nanoparticles)	+	-/ Light intensity measurement	NR	-	-	+	(12)
Capillary-driven (Paper-based)	3	5	-	-	-/-	2	+	-	-	(13)
Capillary-driven	2	5	-	-	-/ Light intensity measurement	NR	-	+	-	(14)
Capillary-driven	3	50	+ (Lysis)	-	-/ Impedance Spectroscopy	2	-	-	+	(15)
Capillary-driven	3	15	+ (Dilution)	-	-/ Dielectrophoresis	15	+	-	-	(16)
Air Actuation	$\geq 2$	30	+ (Dilution)	+	Crystal violet and glacial acetic acid/ Camera Inspection	5	-	-	+	(17)
Syringe pump-driven	2	NR	+ (Lysis)	-	-/ Hydrodynamic focusing & Light scattering	15	-	-	+	(18)
Syringe-pump driven	3	6	-	-	-/ Bifurcation	20	+	-	-	(19)
External pump-driven	2	50	-	-	On-chip lysis and on-chip dilution/ Impedance Spectroscopy	20	-	-	+	(20)
Centrifugal based	$\geq 2$	0.1	-	-	-/ Smart phone-based & Microscopic inspection	10	+	+	+	This study

+/-: Yes/No  
NR: not reported  
HCT: Hematocrit measurement  
WBC: white blood cell concentration measurement

## References

1. Iqbal M, Mukhamedshin A, Lezzar DL, Abhishek K, McLennan AL, Lam FW, et al. Recent advances in microfluidic cell separation to enable centrifugation-free, low extracorporeal volume leukapheresis in pediatric patients. *Blood Transfusion*. 2023;21(6):494.
2. Kuo JN, Chen XF. Plasma separation and preparation on centrifugal microfluidic disk for blood assays. *Microsystem Technologies*. 2015;21:2485–94.
3. Lenz KD, Jakhar S, Chen JW, Anderson AS, Purcell DC, Ishak MO, et al. A centrifugal microfluidic cross-flow filtration platform to separate serum from whole blood for the detection of amphiphilic biomarkers. *Sci Rep*. 2021;11(1):5287.
4. Kinahan DJ, Kearney SM, Kilcawley NA, Early PL, Glynn MT, Ducree J. Density-gradient mediated band extraction of leukocytes from whole blood using centrifugo-pneumatic siphon valving on centrifugal microfluidic discs. *PLoS One*. 2016;11(5):e0155545.
5. Sun Y, Sethu P. Low-stress microfluidic density-gradient centrifugation for blood cell sorting. *Biomed Microdevices*. 2018;20:1–10.
6. Khodadadi R, Eghbal M, Ofoghi H, Balaei A, Tamayol A, Abrinia K, et al. An integrated centrifugal microfluidic strategy for point-of-care complete blood counting. *Biosens Bioelectron*. 2024;245:115789.
7. Yang S, Kim SH, Intisar A, Shin HY, Kang HG, Kim MY, et al. Fully Automated Continuous Centrifugal Microfluidics Isolates Natural Killer Cells with High Performance and Minimal Stress. *Anal Chem*. 2023;95(26):9949–58.
8. Moen ST, Hatcher CL, Singh AK. A centrifugal microfluidic platform that separates whole blood samples into multiple removable fractions due to several discrete but continuous density gradient sections. *PLoS One*. 2016;11(4).
9. Agarwal R, Sarkar A, Bhowmik A, Mukherjee D, Chakraborty S. A portable spinning disc for complete blood count (CBC). *Biosens Bioelectron*. 2020 Feb 15;150.
10. Berry SB, Fernandes SC, Rajaratnam A, DeChiara NS, Mace CR. Measurement of the hematocrit using paper-based microfluidic devices. *Lab Chip*. 2016;16(19):3689–94.
11. Bills M V., Nguyen BT, Yoon JY. Simplified White Blood Cell Differential: An Inexpensive, Smartphone- and Paper-Based Blood Cell Count. *IEEE Sens J*. 2019 Sep 15;19(18):7822–8.
12. Zhang Y, Bai J, Wu H, Ying JY. Trapping cells in paper for white blood cell count. *Biosens Bioelectron*. 2015 Jul 5;69:121–7.
13. Wang X, Lin G, Cui G, Zhou X, Liu GL. White blood cell counting on smartphone paper electrochemical sensor. *Biosens Bioelectron*. 2017 Apr 15;90:549–57.
14. Wang Y, Nunna BB, Talukder N, Lee ES. Microfluidic-Based Novel Optical Quantification of Red Blood Cell Concentration in Blood Flow. *Bioengineering*. 2022 Jun 1;9(6).
15. Mehran A, Rostami P, Saidi MS, Firoozabadi B, Kashaninejad N. High-throughput, label-free isolation of white blood cells from whole blood using parallel spiral microchannels with u-shaped cross-section. *Biosensors (Basel)*. 2021 Nov 1;11(11).
16. Peng T, Su X, Cheng X, Wei Z, Su X, Li Q. A microfluidic cytometer for white blood cell analysis. *Cytometry Part A*. 2021 Nov 1;99(11):1107–13.
17. Murray LP, Mace CR. A Novel Paper-Based Cytometer for the Detection and Enumeration of White Blood Cells According to their Immunophenotype. *Anal Chem*. 2022;29:10443–50.
18. Al-Tamimi M, El-Sallaq M, Altarawneh S, Qaqish A, Ayoub M. Development of Novel Paper-Based Assay for Direct Serum Separation. *ACS Omega*. 2023 Jun 13;8(23):20370–8.
19. Zhu S, Wu D, Han Y, Wang C, Xiang N, Ni Z. Inertial microfluidic cube for automatic and fast extraction of white blood cells from whole blood. *Lab Chip*. 2020 Jan 21;20(2):244–52.
20. Hassan U, Reddy B, Damhorst G, Sonoiki O, Ghonge T, Yang C, et al. A microfluidic biochip for complete blood cell counts at the point-of-care. *Technology (Singap World Sci)*. 2015 Dec;03(04):201–13.